JOURNAL OF VIROLOGY, May 2005, p. 5721–5731 Vol. 79, No. 9
0022-538X/05/$08.00+0 doi:10.1128/JVI.79.9.5721–5731.2005
Copyright © 2005, American Society for Microbiology. All Rights Reserved.

Rapid Viral Escape at an Immunodominant Simian-Human Immunodeficiency Virus Cytotoxic T-Lymphocyte Epitope Exacts a Dramatic Fitness Cost

Caroline S. Fernandez,[1]† Ivan Stratov,[1]† Robert De Rose,[1] Katrina Walsh,[1] C. Jane Dale,[1] Miranda Z. Smith,[1] Michael B. Agy,[2] Shiu-lok Hu,[2] Kendall Krebs,[3] David I. Watkins,[3] David H. O'Connor,[3] Miles P. Davenport,[4] and Stephen J. Kent*

Department of Microbiology and Immunology, University of Melbourne, Victoria 3010, Australia[1]; National Primate Research Centre, University of Washington, Seattle, WA 98105[2]; National Primate Research Centre, University of Wisconsin, Madison WI 53715[3]; and Department of Haematology, Prince of Wales Hospital, and Centre for Vascular Research, University of New South Wales, Kensington, NSW 2052, Australia[4]

Received 8 August 2004/Accepted 6 December 2004

Escape from specific T-cell responses contributes to the progression of human immunodeficiency virus type 1 (HIV-1) infection. T-cell escape viral variants are retained following HIV-1 transmission between major histocompatibility complex (MHC)-matched individuals. However, reversion to wild type can occur following transmission to MHC-mismatched hosts in the absence of cytotoxic T-lymphocyte (CTL) pressure, due to the reduced fitness of the escape mutant virus. We estimated both the strength of immune selection and the fitness cost of escape variants by studying the rates of T-cell escape and reversion in pigtail macaques. Near-complete replacement of wild-type with T-cell escape viral variants at an immunodominant simian immunodeficiency virus Gag epitope KP9 occurred rapidly (over 7 days) following infection of pigtail macaques with $SHIV_{SF162P3}$. Another challenge virus, $SHIV_{mn229}$, previously serially passaged through pigtail macaques, contained a KP9 escape mutation in 40/44 clones sequenced from the challenge stock. When six KP9-responding animals were infected with this virus, the escape mutation was maintained. By contrast, in animals not responding to KP9, rapid reversion of the K165R mutation occurred over 2 weeks after infection. The rapidity of reversion to the wild-type sequence suggests a significant fitness cost of the T-cell escape mutant. Quantifying both the selection pressure exerted by CTL and the fitness costs of escape mutation has important implications for the development of CTL-based vaccine strategies.

A human immunodeficiency virus (HIV) vaccine is urgently needed, and much evidence suggests that HIV-specific T-cell responses should assist in protective immunity. $CD8^+$ cytotoxic T lymphocytes (CTL) partially control high-level viremia during acute HIV infection, while simian immunodeficiency virus (SIV)-specific CTL contribute to the control of chronic infection and protective immunity in macaque models (3, 16, 28). Viral variants selected for the presence of CTL escape mutations commonly emerge and dominate viral quasispecies during the course of HIV infection (1, 21, 22, 25). The evolution of T-cell escape variants, together with neutralizing antibody escape variants (26, 32), likely contributes to the failure to effectively control HIV infection and prevent subsequent immunodeficiency.

Individuals that share major histocompatibility (MHC) alleles have a tendency to also share viral escape variants (21). If HIV is transmitted between hosts with the same MHC class I allele(s), any T-cell escape mutant virus present in the donor will be maintained in the recipient (11, 17). For example, the transmission of HIV type 1 (HIV-1) containing the $CD8^+$ T-cell escape mutation T242N in the Gag TW10 epitope between humans sharing MHC alleles B57/5801 results in the retention of this escape mutation (17). A more pathogenic infection can occur under such circumstances.

In contrast, if CTL escape variants are transmitted to a new host not sharing MHC class I alleles with the donor, the pressure to maintain CTL escape variants is lost (9, 17). In cases in which a CTL escape mutation results in a fitness cost to the virus, reversion of the escape mutant to wild-type (WT) virus may occur (9). The rapidity of reversion likely reflects the fitness costs to the virus, although this has not been studied directly.

Recent studies involving the infection of rhesus macaques with clonal, laboratory-generated escape variants of SIV demonstrated that reversion to wild-type virus occurs in two of three studied epitopes (9). Detailed kinetic studies of infection with T-cell escape viral variants that arise naturally during serial transmission between macaques have not previously been performed. Serial transmission of multiple SIV or simian-human immunodeficiency virus (SHIV) quasispecies between macaques, some of which contain T-cell escape variants arising from in vivo CTL selection, may more closely reflect human-to-human transmission.

We therefore mapped SIV Gag-specific T-cell epitopes in pigtail macaques (*Macaca nemestrina*). An immunodominant $CD8^+$ T-cell epitope, Gag KP9, previously identified (29), was

* Corresponding author. Mailing address: Department of Microbiology and Immunology, University of Melbourne, Victoria 3010, Australia. Phone: 61383449939. Fax: 61383443846. E-mail: skent@unimelb.edu.au.

† Contributed equally to the work.

found in many of the macaques. We then studied the infection of pigtail macaques with $SHIV_{SF162P3}$ and observed rapid viral escape at this epitope in two of three KP9-responding animals. The rate of replacement of wild-type virus with escape mutant virus allows estimation of the fitness benefits of the escape mutation. Since the fitness advantage of escape at a single CTL epitope occurs due to the loss of CTL killing through this epitope, this also allows estimation of the rate of CTL killing of infected cells through a single epitope in vivo.

In contrast to the $SHIV_{SF162P3}$ stock, another challenge virus stock, $SHIV_{mn229}$, was derived by serial transmission between pigtail macaques and had evolved escape mutations in KP9. When this KP9 escape virus stock was inoculated into four pigtail macaques not responding to KP9, rapid reversion to the wild-type virus ensued. The rate of in vivo selection of wild-type SHIV variants reflects the in vivo fitness cost of a T-cell escape mutation. This fitness cost of T-cell escape mutations can therefore be calculated where frequent analyses of SHIV RNA clones containing either wild-type or T-cell escape variants are conducted.

Ultimately, the utility of particular T-cell responses is determined by both the rate of killing of infected cells and the fitness cost of escape mutation at the T-cell epitope. Together, our analysis provides insights into the efficiency of epitope-specific CD8 T-cell responses in controlling primate lentiviruses and the role of viral escape in undermining such control. Vaccine-induced CTL responses are likely to be most efficacious where they select for mutations with the greatest loss of viral fitness.

MATERIALS AND METHODS

Epitope mapping by IFN-γ ELISpot and intracellular cytokine staining. Antigen-specific gamma interferon (IFN-γ) responses were measured in peripheral blood mononuclear cells (PBMC) or whole blood by using ELISpot and intracellular cytokine-staining (ICS) assays, respectively. The monkey IFN-γ ELISpot kit (U-CyTech, Utrecht, The Netherlands) was used as previously described (8). Briefly, PBMC were stimulated with a pool of 125 overlapping 15-mer SIV_{mac239} Gag peptides, individual 15-mer peptides (both kindly made available through the National Institutes of Health [NIH] AIDS Research and Reference Reagent Program), or minimal 8- to 13-mer peptides (Chiron Mimotopes, Clayton, Australia) at 1 μg/ml/peptide for 18 h, washed, and then transferred to anti-IFN-γ monoclonal antibody-coated plates and restimulated for 5 h. Cells were lysed, and wells were incubated with biotinylated anti-IFN-γ polyclonal rabbit antibody, followed by incubation with a gold-labeled antibiotin immunoglobulin G antibody. IFN-γ spots were developed and counted on an automated reader (AID, Strassberg, Germany), and results were normalized to antigen-specific IFN-γ-secreting precursor frequencies per 10^6 PBMC. A positive response was determined to be both >50 spot forming cells/10^6 PBMC greater than the number of background dimethyl sulfoxide (DMSO)-stimulated cells and at least threefold greater than the background response, consistent with reports for other systems (27).

Intracellular IFN-γ secretion was assessed by flow cytometry as previously described (8, 19). In short, 200 μl of whole blood was incubated with peptides, as described above, at 1 μg/ml/peptide, along with costimulatory antibodies anti-CD28 (clone L293) and anti-CD49d (clone L25.3) (BD Biosciences, PharMingen, San Diego, CA) for 2 h at 37°C in 5% CO_2. Antigen processing was then blocked by the addition of 10 μg/ml of brefeldin A (Sigma, St. Louis, MO), and blood was incubated for a further 4 to 5 h. The cells were then stained with anti-CD4-fluorescein isothiocyanate (clone M-T477), anti-CD3-PE (clone SP34) and anti-CD8-PerCP (clone SK1) (BD Biosciences) for 30 min at 4°C. Erythrocytes were then lysed using fluorescence-activated cell sorter lysing solution (BD Biosciences) and washed with phosphate-buffered saline, and the remaining cells permeabilized with fluorescence-activated cell sorter permeabilizing solution (BD Biosciences). Cells were then incubated with anti-IFN-γ-allophycocyanin (clone B27; BD Biosciences) and formaldehyde fixed before acquisition (BD FACScalibur). Antigen-specific $CD8^+$ T-cell or $CD4^+$ T-cell responses were assessed as the percentages of $CD3^+CD8^+$ or $CD3^+CD4^+$ cells expressing IFN-γ levels greater than those of DMSO control-stimulated cultures. Positive responses were those that were at least three times the background response to DMSO alone and were ≥0.10%.

MHC class I allele discovery and reference strand-mediated conformation analysis (RSCA). To identify whether macaques in which the $SHIV_{mn229}$ virus was passaged were capable of presenting the KP9 epitope, we studied the MHC class I molecules in cDNA from frozen PBMC for the *M. nemestrina* allele *Mane-A*10*, which we have previously shown to present KP9 (29). We also analyzed expression of Mane-A*16, which differs from Mane-A*10 by only a single amino acid (29). First-strand cDNA was created from total *M. nemestrina* blood RNA (extracted using a QIAamp RNA blood mini kit; QIAGEN, Hilden, Germany) in a two-step reaction containing $oligo(dT)_{12-18}$ (Invitrogen, Carlsbad, CA), 2.5 mM concentrations of each dNTP (Promega, Madison, WI), dithiothreitol (Invitrogen), RNasin (Promega), 5× first-strand buffer, and SuperScript III RNase H^- reverse transcriptase (Invitrogen). The reaction conditions were 65°C for 5 min, 42°C for 2 min (pause), 42°C for 50 min, and 70°C for 15 min, using a GeneAmp 9700 PCR thermal cycler (Applied Biosystems, Foster City, CA).

Full-length *M. nemestrina* MHC class I alleles were amplified from the cDNA by using a 25 μM concentration of primer set 5′ALoci (5′-TCACACTTTACA AGCCGTGAGAGACAC-3′) and 3′ALoci (5′-ATGGCGCCCCGAACCCTC-3′) (A loci), 5′A*10tet (5′-GGGCATATGGGCTCGCACTCCATGAGG-3′) and 3′A*10tetstop (5′-CCCTGGATCCCTAGGAAGACGGCTCCCATCTC-3′), or 5′BLoci (5′-TCATGGCGCCCCGAACCCTC-3′) and 3′BLoci (5′-TCA AGCCGTGAGAGACWCATCAGAGCC-3′) (B loci), designed based on rhesus macaque MHC class I sequences (23). Amplicons were generated by using Platinum Pfx DNA polymerase (Invitrogen) for 20 cycles (94°C for 1 min, 65°C for 1 s, and 69°C for 90 s) or Phusion high-fidelity DNA polymerase (Finnzymes, Espoo, Finland) for 25 cycles. The amplified MHC class I DNA was purified from a 1% agarose gel by using the QIAquick gel extraction kit (QIAGEN) according to the manufacturer's instructions. To isolate individual MHC class I genes, amplicons were then ligated into pCR2.1 (Invitrogen) or pGEM-T easy vectors (Promega) and transformed into *Escherichia coli* TOP10 or JM109. Individual clones from the transformation were isolated and purified according to the QIAGEN QIAprep protocol. Each MHC-containing plasmid was sequenced in its entirety in BigDye Terminator v3.1 (Applied Biosystems) or DYEnamic ET Terminator (Amersham Biosciences) reactions primed by synthetic oligonucleotides annealed to the vector on both sides of the insert. Sequences were run on an ABI 3730 instrument, and the sequence chromatograms were edited in Sequencher 4.1 (Gene Codes, Ann Arbor, MI). The edited sequences were aligned to all previously described pigtail macaque MHC class I alleles.

The RSCA method to characterize *M. nemestrina* MHC molecules was adapted from similar methods for the detection of rhesus macaque (J. Weinfurter et al., unpublished data) and human MHC alleles (2, 29). Approximately 700 bp of MHC class I cDNA spanning exons 2 and 3 (encoding the peptide-binding regions) were amplified from pigtail macaque cDNA, using the 5′RSCA (5′-GCTACGTGGAYGAYACGC-3′) and 3′RSCA (5′-CARAAGGCACMW CCACAGC-3′) primers as described above, for 35 cycles with *Taq* Hi Fi DNA polymerase (Invitrogen). Rhesus macaque reference strands Mamu-B*07, Mamu-B*60, Mamu-B*05, Mamu-A*15, and Mamu-A*20 were PCR amplified under the same conditions, except that 5′RSCA primer was replaced with 5′-end-labeled Cy5-5′RSCA. RSCA reactions to form heteroduplexes between the reference strands and unknown MHC alleles were performed under the following conditions: 95°C for 4 min, 55°C for 5 min, and 15°C for 5 min. The product was run on a nondenaturing polyacrylamide gel for 7 h, along with external size standards, on an AlfExpress DNA analyzer (Amersham Biosciences, Piscataway, NJ) according to the manufacturers' instructions. An allele's migration rate in the gel was dictated by the conformation of the heteroduplex formed by the unknown allele and a particular reference strand. Identical alleles shared between macaques have the same mobility when heteroduplexed to the same reference strand. Occasionally, the conformational heteroduplex of distinct alleles will have identical mobility, so each cDNA sample is hybridized separately to multiple reference alleles to verify RSCA results. The presence of a particular allele within a total cDNA population was confirmed by comparing it to the mobility of cloned MHC alleles run on the same gel.

SHIV and passage history. The $SHIV_{SF162P3}$ virus, passaged in rhesus macaques (*Macaca mulatta*), was obtained from the NIH AIDS Reagent and Reference Repository and amplified on human PBMC prior to infecting pigtail macaques (8, 12, 13).

The $SHIV_{mn229}$ was derived from $SHIV_{HXB2}$, a chimeric virus containing the SIV_{mac239} backbone and $HIV\text{-}1_{HXB2}$ vpu/env/tat/rev (8, 18). Prior to 1995, the molecular clone was first used to infect 10 naïve pigtail macaques at the Uni-

versity of Washington (see Fig. 4). Eight of these 10 macaques infected with this molecular clone completely controlled viremia to $\leq 10^2$ RNA copies/ml of plasma, but 2 of these 10 pigtail macaques developed sustained SHIV RNA levels of $>10^4$ copies/ml and later developed disease with severe depletion of CD4 T cells (at week 70 for animal 93099 and week 15 for animal 90044). A 10-ml aliquot of blood from each of these two animals with progressive SHIV infection was used to infect two naïve pigtail macaques (95229 and 95221), both of which developed rapid complete depletion of CD4 T cells (by 2 to 3 weeks) and high SHIV RNA levels. The $SHIV_{mn229}$ strain was derived from bone marrow cultures of animal 95229 and has subsequently been used as a pathogenic SHIV strain in pigtail macaques (8, 30, 31). Samples of frozen PBMC and plasma stored for 7 years from animals 95229, 95221, and 93099 were used to extract RNA for analyses of the SIV Gag sequence and MHC class I alleles by RSCA. No viable samples from animal 90044 (involved in the first passage) were available.

Both the $SHIV_{SF162P3}$ and $SHIV_{mn229}$ stocks were then used in challenge experiments with pigtail macaques sequentially immunized with DNA and recombinant fowlpox virus (rFPV) vaccines expressing shared SIV_{mac239} Gag antigens as previously described (8, 15). This general DNA prime/poxvirus boost vaccination approach provides partial protection from CD4 T-cell decline and SHIV viremia in rhesus macaque models, and we observed similar results by using DNA and rFPV prime/boost strategies in pigtail macaques (7). $SHIV_{SF162P3}$ was administered atraumatically intravaginally by using 6×10^3 50% tissue culture infective doses in divided doses over 2 days. $SHIV_{mn229}$ was administered atraumatically intrarectally by using 10^5 50% tissue culture infective doses in divided doses over 2 days.

Cloning and sequencing of plasma SHIV RNA. SHIV RNA from pigtail macaque plasma and each of the SHIV challenge stocks were extracted as previously described (8). First-strand cDNA was generated in a two-step reaction mixture containing a 1.25 μM concentration of random hexamers (Invitrogen, Carlsbad, CA), 500 μM concentrations of each dNTP (Promega, Madison, WI), 5 mM dithiothreitol (Invitrogen), RNasin (Promega), 5× first-strand buffer, and SuperScript III RNase H^- reverse transcriptase (Invitrogen) according to the manufacturer's instructions (Invitrogen). The reaction conditions were as follows: 65°C for 5 min, pause on ice for 2 min, 25°C for 10 min, 42°C for 45 min, and 70°C for 15 min, using a GeneAmp 9700 PCR thermal cycler (Applied Biosystems, Foster City, CA). The first-strand cDNA was then incubated with 2 U of RNase H at 37°C for 20 min.

PCR amplification of $SHIV_{mn229}$ or $SHIV_{SF162P3}$ challenge stock cDNAs were performed using SIV Gag-specific primer pairs as follows: primer no. 2 (5′ TTAGCAGAAAGCCTGTTGGA 3′) and primer no. 3 (5′ AGAGAGAATT GAGGTGCAGC 3′) were used to give a 1,380-bp fragment; primer no. 9 (5′ AACTCCGTCTTGTCAGGG 3′) and primer no. 5 (5′ GTTCCTGCA ATRTCKGATCC 3′) were used to give a 703-bp fragment; and primer no. 4 (5′ CACGCAGAAGAGAAAGTGAA 3′) and primer no. 5 (5′ GTTCCTGC AATRTCKGATCC 3′) were used to give a 451-bp fragment. Pigtail macaque plasma $SHIV_{mn229}$ or $SHIV_{SF162P3}$ cDNA was PCR amplified using SIV Gag-specific primer pair of primer no. 4 and primer no. 5 described above. PCR was done using one of two thermostable DNA polymerases, Phusion high-fidelity DNA polymerase (Finnzymes) or Elongase DNA polymerase (Invitrogen), according to the respective manufacturer's instructions. PCR conditions using Phusion DNA polymerase were 98°C for 30 s, followed by 35 cycles of 98°C for 10 s, 56°C for 20 s, and 72°C for 30 s, and a final cycle of 72°C for 7 min, while reaction conditions for Elongase DNA polymerase were 94°C for 1 min, followed by 35 cycles of 94°C for 30 s, 55°C for 30 s, and 68°C for 30 s, and a final cycle of 68°C for 10 min. Where necessary, a second round of PCR amplification was done using the same primer pair on 0.4% of the primary product as the template.

Amplicons were ligated into pGEM-T easy vector system (Promega) and transformed into *E. coli* JM109 (Promega) competent cells according to the manufacturer's instructions. Individual clones were sequenced across the insert by using either the BigDye Terminator v3.1 (Applied Biosystems) or the DYEnamic ET Terminator (Amersham Biosciences) chemistry.

Estimation of selection pressure. Viral strains compete with each other within a host, and the clone with the highest fitness comes to dominate. Whenever we observe the replacement of one clone by another, we can infer a fitness advantage of the new clone. The rate at which the new mutant "outgrows" the old allows us to estimate the growth advantage of the new mutant. Thus, when we see replacement of wild-type virus by T-cell escape mutant virus or vice versa, we can estimate the fitness benefits or fitness costs of escape. The absolute difference in growth rates between two viral strains over a time period can be estimated directly from the proportion of clones of each strain present at the beginning and the end of the time period. That is, if $f_a(t)$ is the fraction of clones of type a at time t and $f_b(t)$ is the fraction of clones of type b, then the absolute difference in growth rates between strains a and b (i.e., $g_a - g_b$) over the period from t_1 to t_2 can be estimated with the following equation: $g_a - g_b = \{(\ln [f_a(t_2)] - \ln [f_a(t_1)]) - (\ln [f_b(t_2)] - \ln [f_b(t_1)])\}/(t_2 - t_1)$, where ln is the natural logarithm. The absolute difference in growth rates is not equivalent to the traditional concept of a selection coefficient (4). This is a minimum estimate of the difference in growth rates between the two strains, since it assumes exponential growth of both strains. However, in a number of circumstances, the real difference in exponential growth rate between the two strains may be reduced (due to, for example, slowing of growth around the peak of viremia due to target cell limitation).

In circumstances in which n clones were sequenced at a given time point but no clones of a particular strain were observed, we used the conservative assumption that the real frequency of the strain was $1/n$. This, again, has the tendency to underestimate the difference in growth rates.

RESULTS

Epitope mapping of T-cell responses in *M. nemestrina*. To identify potential sites of T-cell escape, we first mapped T-cell epitopes to SIV Gag in two vaccine studies in which pigtail macaques (*M. nemestrina*) were primed with DNA and rFPV vaccines and challenged with either $SHIV_{SF162P3}$ or $SHIV_{mn229}$. We used both IFN-γ ELISpot and ICS assays to rapidly screen for responses across multiple peptide pools. The responses were confirmed with the two separate assays where possible, and the phenotypes of the responding cells were analyzed using ICS. A conservative designation of T-cell epitopes was employed, whereby results were considered positive only if they were (i) confirmed by both IFN-γ ELISpot and ICS assays, (ii) found in multiple animals, or (iii) a case in which a positive result was mapped to two adjacent peptides.

Twenty-nine epitope-specific T-cell responses were identified by using the criteria described above (Table 1). The majority (24 of 29) of T-cell responses were phenotyped, 18 (75%) were CD8 T-cell epitopes, and 6 (25%) were CD4 T-cell epitopes. Nine of the stronger T-cell responses had minimal epitopes, defined by use of truncated peptides. An example in which a strong CD8 T-cell response was mapped by IFN-γ ELISpot is shown in Fig. 1. By far, the most commonly recognized Gag peptide was peptide 161-175, mapped to the $KP9_{164\text{-}172}$ nonamer we have previously described (29). The KP9-specific response is present in animals encoding the MHC class I allele *Mane-A*10*, and we have previously shown that Mane-A*10 restricts KP9-specific CD8 T cells (29).

CTL pressure results in rapid mutation at KP9. We studied immune responses and virus sequence evolution in DNA and rFPV-immunized pigtail macaques challenged with $SHIV_{SF162P3}$, a challenge stock containing SIV_{mac239}-derived Gag and previously passaged in rhesus macaques (*M. mulatta*) (12, 13). To confirm the presence of the KP9 epitope, 18 clones were sequenced across the KP9 epitope from the $SHIV_{SF162P3}$ stock, and all contained wild-type SIV_{mac239} sequences. Three animals responding to the KP9 T-cell epitope and five animals not responding to this epitope were identified. Plasma virus RNA samples from these animals taken early (1 to 4 weeks) and up to 11 weeks after challenge with $SHIV_{SF162P3}$ were sequenced across the KP9 epitope (Fig. 2). Two of the three animals responding to the KP9 epitope after vaccination generated T-cell escape variants at weeks 2.5 and 3 (Fig. 2A; expressed as a proportion of clones wild type at KP9 in Fig. 2B). None of the five animals not responding to KP9 generated T-cell escape variants up to 11 weeks after infection. Interestingly, in both of the KP9-responding animals generating T-cell

TABLE 1. $CD8^+$ or $CD4^+$ T-cell epitopes mapped to SIV Gag

SIV Gag peptide[a]	Animal no.	Phenotype	% Cells expressing IFN-γ[b]	SFC/10^6 PBMC[b]	Minimal epitope
1-15/5-19	3790	CD8	0.17		
	4277	CD8	0.47		
	4295			165	
	4296			175	
13-27/17-31	4277	CD4	0.67	120	EKIRLRPNGKKKY
	4295	CD4		105	
	4296	CD4		210	
25-39	4293	CD8	7.90	1,620	KYMLKHVVW
	4296	CD8	2.98	375	
	4648	CD8	0.80	360	
	4658	CD8	0.40		
37-51/41-55	4295	CD8	1.20	245	
	4296			110	
53-67/57-71	4277	CD8	1.40		
	H21	CD8	0.47		
81-95/85-99	4247	CD8	1.23	105	
	4290	CD8	0.23	190	
	4296			160	
109-123	4290			140	
	4296			210	
137-151/141-155	4250	CD8	0.25		GNYVHLPL
	4666	CD8	2.29	540	
141-155	4245	CD4	0.40	130	GGNYVHLPLSP
161-175	3790	CD8	1.70		KKFGAEVVP
	4241	CD8		107	
	4246	CD8	18.71	1,405	
	4247	CD8	8.50	362	
	4254	CD8	4.60		
	4277	CD8	5.10	220	
	4290	CD8	4.30	115	
	4292	CD8	3.90	180	
	4295	CD8	5.90	357	
	4296	CD8	1.20	250	
	4299	CD8		165	
	4380	CD8	0.70	180	
	4382	CD8	0.10	95	
	4386	CD8	0.90	65	
	4664	CD8	9.00	320	
	4668	CD8	6.20	440	
	H8	CD8	4.40	660	
177-191/181-195	4290	CD8	0.45		
	4666	CD8	0.53		
189-203	4290	CD8	6.48		
	4666	CD8	0.91		
189-203/193-207	4277	CD4	0.17		
197-211/201-215	4246	CD4	0.32	210	
	4254	CD4	0.36		
	H21	CD4	0.18		
205-219	1.7105	CD8	0.10	115	
245-259/249-263	4293	CD8	7.80	1,645	YRQQNPIP
	4295	CD8	3.90	215	
265-279/269-283	4237	CD8	0.77		
	4238	CD8	0.41		
301-315/305-319	1.7105	CD8	0.19	190	
309-323/313-327	4277	CD4	0.38		
	4664	CD4		220	
321-335	4290	CD8	0.23	105	
	4296			245	
321-335/325-339	4246	CD4	0.70	65	IQNANPDCKLVLK
353-367	1.7105			290	
	4296			185	
365-379/369-383	4240	CD8	10.79	1,130	ALAPVPIPF
	4253	CD8	0.61	205	
385-399/389-403	4386			315	
413-427/417-431	4532	CD8	5.14		CGKMDHVM
433-447/437-451	4666	CD8	0.54		
441-455/445-459	4668			140	
453-467/457-471	4259	CD8	0.14		
469-483/473-487	4668			130	

[a] Peptides are 15-mer overlapping by 11 amino acids. Numbers indicate amino acid residues. Some epitopes span two adjacent peptides.
[b] Intracellular cytokine-staining and ELISpot responses show the maximum response detected in each animal. SFC, spot-forming cells.

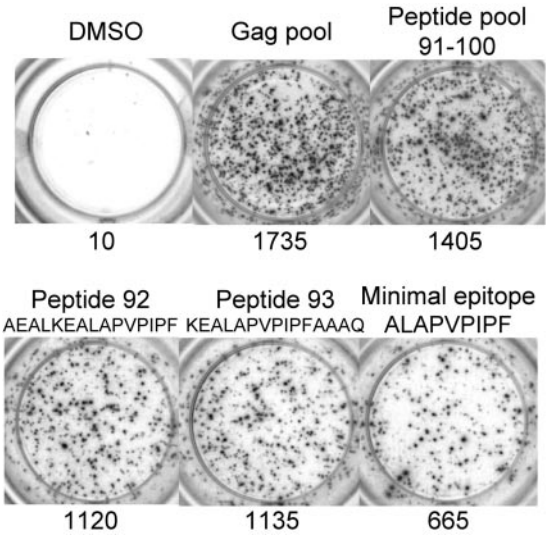

FIG. 1. Mapping of a minimal pigtail macaque T-cell epitope. Epitope AF9 was identified by IFN-γ ELISpot assay using smaller pools of SIV Gag peptides and individual and truncated peptides. Numbers indicate IFN-γ spot-forming cells per million PBMC.

escape mutations, the K165R mutation at position 2 was preceded by a minor population with the P172S mutation at position 9, although the K165R mutation dominated viral quasispecies by week 11 postchallenge.

To examine whether the mutations in KP9 were truly T-cell escape variants, the binding avidity of fresh blood cells from a KP9-responding macaque was studied for the recognition of peptides derived from the wild-type and mutant virus sequences, containing the K165R and/or the P172S mutations identified above (Fig. 3). Diminished recognition of all the mutant peptides in comparison to the wild-type peptides was observed at all concentrations of peptides examined, consistent with positions 2 and 9 being common anchor residues. The K165R mutation had a more profound effect on T-cell recognition than the P172S mutant.

Serial passage of $SHIV_{mn229}$ results in T-cell escape at KP9. As discussed above, the $SHIV_{SF162P3}$ virus stock, passaged previously in rhesus macaques, was wild type at KP9. When we studied another challenge virus, $SHIV_{mn229}$, we found that the wild-type sequence at the KP9 epitope was almost totally replaced (40 of 44 clones sequenced) with the same K165R mutation observed to arise during acute infection with $SHIV_{SF162P3}$.

It seemed plausible that passage of the original $SHIV_{mn229}$ virus stock through pigtail macaques sharing the same MHC class I allele presenting KP9 could explain the K165R mutation observed. The $SHIV_{mn229}$ was derived in the mid-1990s from serial passage of an initially nonpathogenic SIV_{mac239}/$HIV\text{-}1_{HXB2}$ chimeric molecular clone, first through two pigtail macaques (90044 and 93099), resulting in disease onset at weeks 15 and 70, respectively, and then through a third pigtail macaque (95229), which developed rapid CD4 T-cell depletion. Another pigtail macaque (95221) also received blood from the first passage and developed rapid CD4 depletion, as have all subsequent naïve pigtail macaques infected with the final $SHIV_{mn229}$ stock (8). Frozen plasma RNA samples were available from three of these four animals for SIV Gag sequencing across the KP9 epitope. The first passage through animal 93099 resulted in the acquisition of a proline-to-serine mutation at position 9 (P172S) (Fig. 4). Virus derived following the second passage through animal 95229 maintained a minor variant with the P172S mutation; however, most clones sequenced had now acquired the K165R mutation observed in the final $SHIV_{mn229}$ stock. Interestingly, this sequence of mutations (P172S early followed by K165R later) was also observed in both of the animals with T-cell escape following $SHIV_{SF162P3}$ challenge (Fig. 2).

To determine whether the pigtail macaques through which the $SHIV_{mn229}$ was passaged were capable of presenting the KP9 epitope, we studied MHC class I RNA from PBMC frozen for over 7 years. We have previously determined that the pigtail macaque MHC class I molecule Mane-A*10 presents the KP9 epitope (29). MHC class I cDNA from the three macaques with available samples (93099, 95229, and 95221) were studied by a novel RSCA technique (Fig. 5). This technology utilizes fluorescent rhesus MHC class I alleles to heteroduplex pigtail MHC class I cDNA. Each heteroduplexed MHC class I allele runs at a unique mobility on nondenaturing gels. Animal 93099, involved in the first passage with slow development of disease, had an MHC class I heteroduplex peak running with identical mobility to cloned *Mane-A*10*. Interestingly, animals 95229 and 95221, involved in the second passage that was acutely pathogenic, did not encode the *Mane-A*10* allele. We have also previously identified another MHC class I allele, *Mane-A*16*, which differs from *Mane-A*10* by only two nucleotides, that was present in a KP9-responding animal without *Mane-A*10* (29). This suggests that *Mane-A*16* or, less likely, a linked allele also presents KP9. We studied the animals in which $SHIV_{mn229}$ was passaged, but none of the animals had an MHC class I heteroduplex peak corresponding to cloned *Mane-A*16* (data not shown).

Maintenance and reversion of T-cell escape at the immunodominant KP9 epitope. The $SHIV_{mn229}$ challenge stock, 91% of which contained the K165R T-cell escape mutation, was administered to pigtail macaques previously vaccinated with DNA and rFPV vaccines. The immunologic and virologic characteristics of the animals studied are shown in Table 2 (7). Through IFN-γ ELISpot and ICS assays (Table 1), challenged animals were identified responding to KP9 prior to or early after challenge, and the presence of the restricting *Mane-A*10* allele was confirmed by sequencing and RSCA. Six animals responding to the KP9 T-cell epitope and four animals not responding to this epitope had serial plasma virus RNA samples (early and late after challenge with $SHIV_{mn229}$) sequenced across the KP9 epitope (Fig. 6). The K165R mutation was maintained in all clones sequenced from all six KP9 responders challenged with $SHIV_{mn229}$ beyond week 36 postchallenge. In stark contrast, the K165R mutation was rapidly lost from viral clones within 2 weeks in all four KP9 nonresponders challenged with the same virus.

To determine the immunologic impact of reversion at this SIV Gag epitope, serial samples from vaccinated pigtail macaque 4290, a *Mane-A*10*-positive, KP9-responding animal, were analyzed for T-cell responses following challenge with the KP9 escape $SHIV_{mn229}$ challenge stock. The CD8 T-cell response to the KP9 epitope, but not total SIV Gag response,

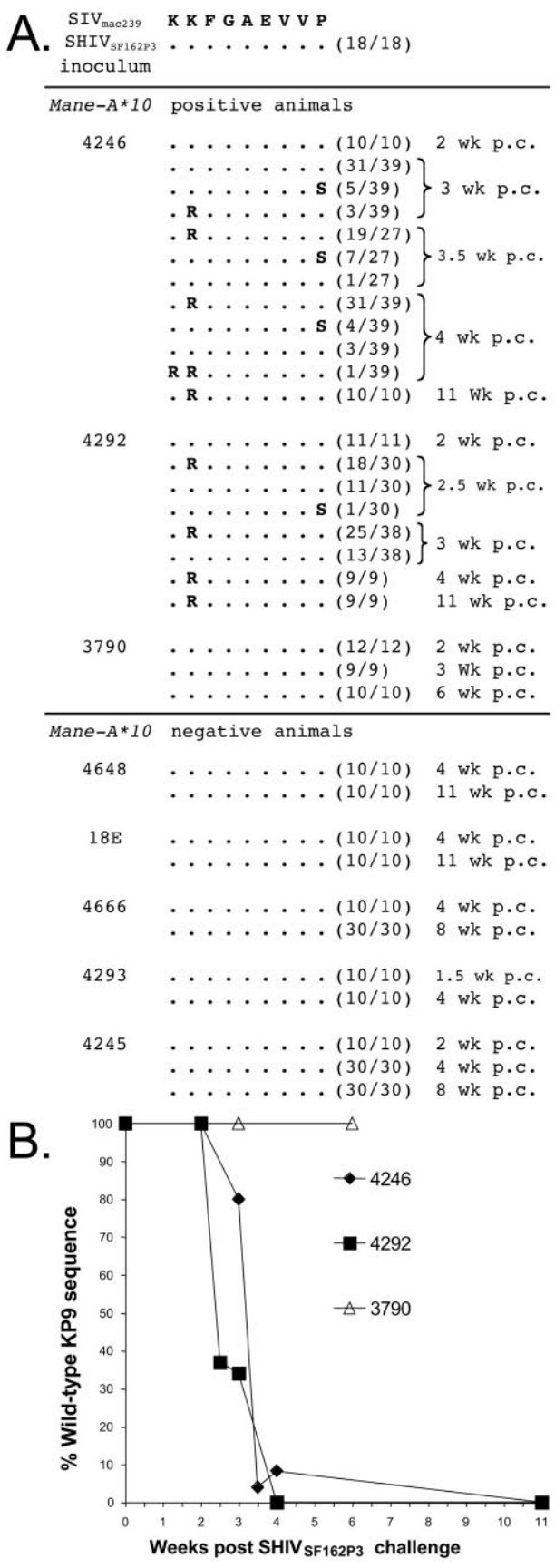

FIG. 2. Escape at SIV Gag KP9 epitope following $SHIV_{SF162P3}$ challenge. (A) Predicted amino acid sequences across the KP9 epitope in multiple clones isolated at early and late time points postchallenge (p.c.) with plasma $SHIV_{SF162P3}$ virus from KP9-responding animals showing escape at K165R mutation at position 2 in two of three animals (top panel) or KP9-nonresponding animals showing maintenance of wild-type KP9 sequence (bottom panel). (B) Graphical representation of the selection pressure in three KP9 responders. Proportions of wild-type clones present at time points postchallenge are shown.

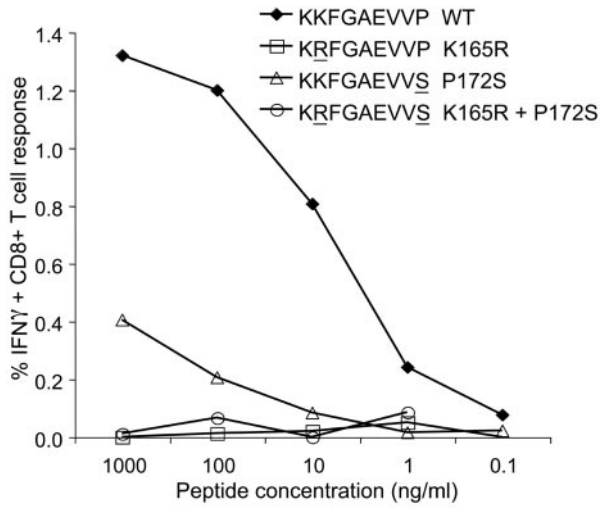

FIG. 3. Lack of T-cell recognition of KP9 mutants. Shown are CD8 T-cell responses (positive for IFN-γ expression [IFNγ+]) to serial dilutions of wild-type peptide KKFGAEVVP and mutant peptides KRFGAEVVP, KKFGAEVVS, and KRFGAEVVS (mutations underlined) in KP9-responding animal 5424 infected with SIV_{mac251}.

was lost over time (Fig. 7). This suggests that the loss of the KP9 epitope led to a subsequent loss of the corresponding epitope-specific T-cell response over time. In two other *Mane-A*10*-positive animals (4277 and 4295) challenged with $SHIV_{mn229}$ for which maintenance of the K165R escape mutation occurred at KP9, a greatly diminished although not completely absent KP9 response was also observed (data not shown).

Estimating killing rate of KP9-expressing cells. Infection of KP9-responding animals with $SHIV_{SF162P3}$ (bearing the wild-type epitope in 18/18 clones sequenced) led to the evolution of escape mutations during acute infection in two of three animals (Fig. 2). The rapid selection of the K165R virus during acute infection allows an estimation of the selection pressure exerted by KP9-specific CTL. In animal 4246, the proportion of WT clones went from 31/39 at day 21 to 1/27 at day 25, and in animal 4292, the proportion of WT clones went from 11/11 to 11/30 at day 14 through day 18. These rates of replacement of WT virus indicate that WT virus has growth disadvantages of 1.15 per day and 0.71 per day, respectively, relative to the escape mutant virus (see Materials and Methods). These growth disadvantages occur because of the CTL killing of WT-infected cells by KP9-specific CTL. Looking at this the other way around, K165R mutant virus had a growth advantage of ~0.93 per day compared to WT virus because of pressure of

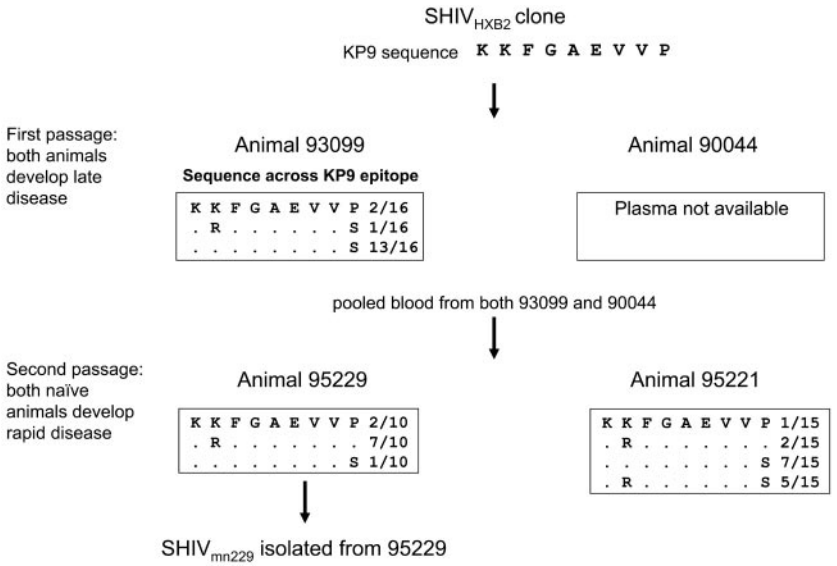

FIG. 4. T-cell escape mutants arise during passage of SHIV$_{mn229}$ virus. Multiple clones of pigtail macaque plasma SHIV cDNA were sequenced across the KP9 epitope during two in vivo passages of the SHIV$_{HXB2}$ molecular clone.

the KP9-specific CTL response on WT virus. However, this growth advantage is a minimal estimate of the true pressure of CTL on WT virus, both because it assumes constant exponential growth and because it ignores any fitness costs of the escape mutation. That is, we are able to measure only the net growth advantage of the escape mutant virus. This most likely includes a growth disadvantage of the escape mutant (see below) as well as the growth benefit of the escape mutation because it is not targeted by KP9-specific CTL. If the K165R virus inherently grows more slowly than the WT virus, then the killing rate of WT virus must be even higher to produce the observed net difference in growth rates.

Estimating the fitness cost of the K165R mutation. The SHIV$_{mn229}$ challenge stock carries predominantly the K165R mutation at the KP9 epitope (40/44 clones sequenced). Infection of KP9-nonresponding animals with SHIV$_{mn229}$ resulted in the rapid reversion of this virus to WT sequence. The difference in growth rates of WT and K165R strains in the absence of CTL pressure can be estimated from the change in the proportion of WT virus observed in the KP9 nonresponders from infection to 2 weeks postinfection. The proportion of WT clones went from 9.1% of clones in the initial inoculum to a mean of 95.5% of clones at 2 weeks in the four KP9 nonresponding animals. (Fig. 6A; expressed as the proportion of

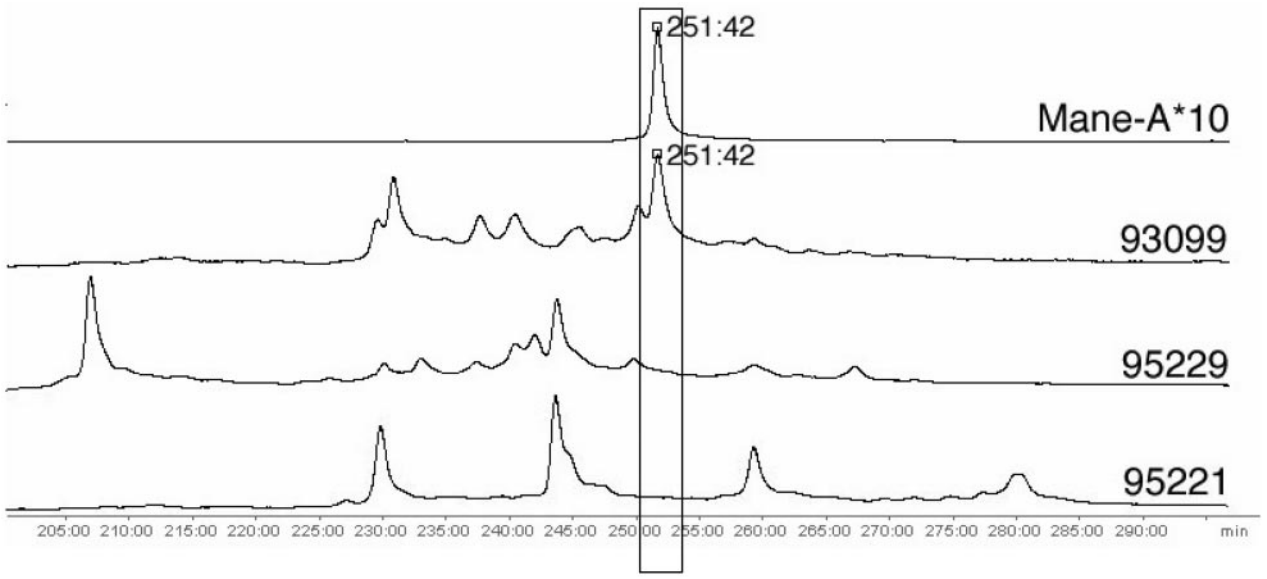

FIG. 5. MHC class I alleles in pigtail macaques in which SHIV$_{mn229}$ was passaged. Shown are results from a reference strand-mediated conformational analysis of in vivo-passaged pigtail macaques' cDNA compared with a clone of the *Mane-A*10* MHC class I allele which presents the KP9 epitope. Peak numbers represent the time (minutes) of migration of the MHC class I heteroduplex through the nondenaturing gel.

TABLE 2. Immunologic and virologic characteristics of DNA/FPV-vaccinated animals studied for reversion of T-cell escape mutation following $SHIV_{mn229}$ challenge

Animal no.	Vaccinated	KP9 responder/*Mane-A*10* positive	Peak Gag-specific CD8 T-cell responses (%)		SHIV viral load postchallenge (log_{10} copies/ml of plasma)		Postacute set point CD4 T-cell count (% lymphocytes at wk 11)
			Prechallenge	Post challenge	Peak (wk 2)	Postacute set point (wk 11)	
4277	Yes	Yes	4.7	9.5	7.03	5.00	14.51
4290	Yes	Yes	2.3	8.6	7.85	5.10	5.74
4382	Yes	Yes	1.2	2.6	5.88	5.21	4.93
4247	Yes	Yes	1.6	5.0	6.21	4.17	16.85
4386	Yes	Yes	0.2	9.5	4.41	4.07	19.56
4299	Yes	Yes	0.2	5.7	6.20	4.42	26.86
1.7105	Yes	No	0.3	3.0	7.29	5.12	1.10
4194	No	No	0.0	0.1	8.29	5.43	3.65
H20	Yes	No	0.5	5.2	7.17	4.44	14.52
H21	Yes	No	0.4	8.8	4.60	<3.20	24.79

clones wild type at KP9 in Fig. 6B). Assuming exponential growth over this 2-week period, this corresponds to the WT virus having a mean 0.38-per-day (range, 0.34 to 0.42 per day)-higher growth rate than the K165R mutant in the absence of CTL. This growth disadvantage of the K165R mutation relative to the WT virus in the absence of CTL pressure is equivalent to the fitness cost of the escape mutation and is around 0.38 per day. Again, this is a minimal estimate of the true difference in growth rates between the two strains and indicates that the ratio of WT to K165R mutants would double approximately every 2 days in vivo.

DISCUSSION

This report identifies multiple SIV Gag CD8 and CD4 T-cell epitopes in pigtail macaques and focuses on viral escape and reversion at the immunodominant CD8 T-cell epitope KP9 present in the majority of animals studied. Infection of KP9-responding macaques with virus carrying the intact KP9 epitope results in rapid selection of the K165R escape mutant virus. By contrast, in KP9-nonresponding animals the WT sequence is maintained. Challenge of animals responding to KP9 with the KP9 escape $SHIV_{mn229}$ strain derived from serial in vivo passage through pigtail macaques resulted in maintenance of the KP9 mutation. Challenge of animals not capable of responding to KP9 with the strain mentioned above resulted in rapid reversion to wild type. The rapid reversion to wild-type virus in the absence of CTL pressure allows an estimate of the very significant fitness cost associated with the K165R mutation. The reduced fitness of the K165R mutant virus has been confirmed in preliminary in vitro replication studies of the $SHIV_{mn229}$ challenge stock, in which a steady rise in the frequency of wild-type variants, in comparison to the mutant variant, is observed over time in culture (data not shown). The calculations from our in vivo studies suggest the fitness pressure is ~0.38 per day, leading to a doubling of the ratio of WT to K165R virus every ~2 days.

The rate of CTL killing of infected cells through an individual T-cell epitope is not known in SHIV or HIV infection. The rapid selection of escape mutant virus at 2.5 to 3 weeks after infection of KP9-responding animals with $SHIV_{SF162P3}$ allows estimation of the growth disadvantage of KP9 (WT)-bearing cells versus non-KP9-bearing (K165R) infected cells. This growth disadvantage occurs due to the increased CTL killing of KP9-bearing cells compared to non-KP9-bearing cells. Therefore, the difference in growth rates between WT virus and K165R virus provides an estimate of the rate of killing through the KP9 epitope. However, the experimentally observed growth disadvantage of WT virus includes a balance of increased killing of WT-infected cells by KP9-specific CTL and the substantial fitness cost of the K165R escape mutation. The observed growth disadvantage of WT virus in KP9-responding animals (~0.93 per day) is equal to the rate of CTL killing through the KP9 epitope minus the fitness cost of the K165R escape mutation (~0.38 per day). Thus, the rate of CTL killing through the KP9 epitope is ~1.31 per day (0.93 plus 0.38 per day), equivalent to a half-life of WT-infected cells to be killed by KP9-specific CTL of around 12.7 h.

Using the same approach described here, we have also analyzed the rate of replacement of wild-type virus with escape mutant virus from previously published studies (Table 3). Because we do not have estimates of the fitness costs of the escape mutations in these cases, we are able to measure only the net benefits of the escape mutations. For example, Allen et al. (1) saw a shift from 0/37 clones bearing escape mutations at the Tat SL8 epitope to 16/17 bearing mutations between weeks 2 to 4 after infection. This corresponds with an estimated net growth advantage for escape mutant virus of ~0.45 per day, corresponding to a half-life of killing through this epitope of ~37 h. Similar estimates of the rates of CTL killing of WT virus in chronic SHIV infection (3) and acute HIV infection (5, 6) (Table 3) are difficult to compare because of the wide time sampling in these studies. Thus, these estimates for the half-life of CTL killing represent a maximum value and are not inconsistent with the values estimated in our study which employed more-frequent sampling.

The escape of $SHIV_{mn229}$ at the KP9 epitope as a result of serial in vivo passage is intriguing. Although viable cells were not available for T-cell assays from the animals in which this virus was passaged, at least one of the animals (93099) encoded an MHC class I allele (*Mane-A*10*) capable of presenting KP9. Serial virus sequences demonstrate a position 9 mutation (P172S) in the epitope in the first passage and the subsequent presence of the position 2 change (K165R) in animals receiving the second challenge. Interestingly, even though there was a

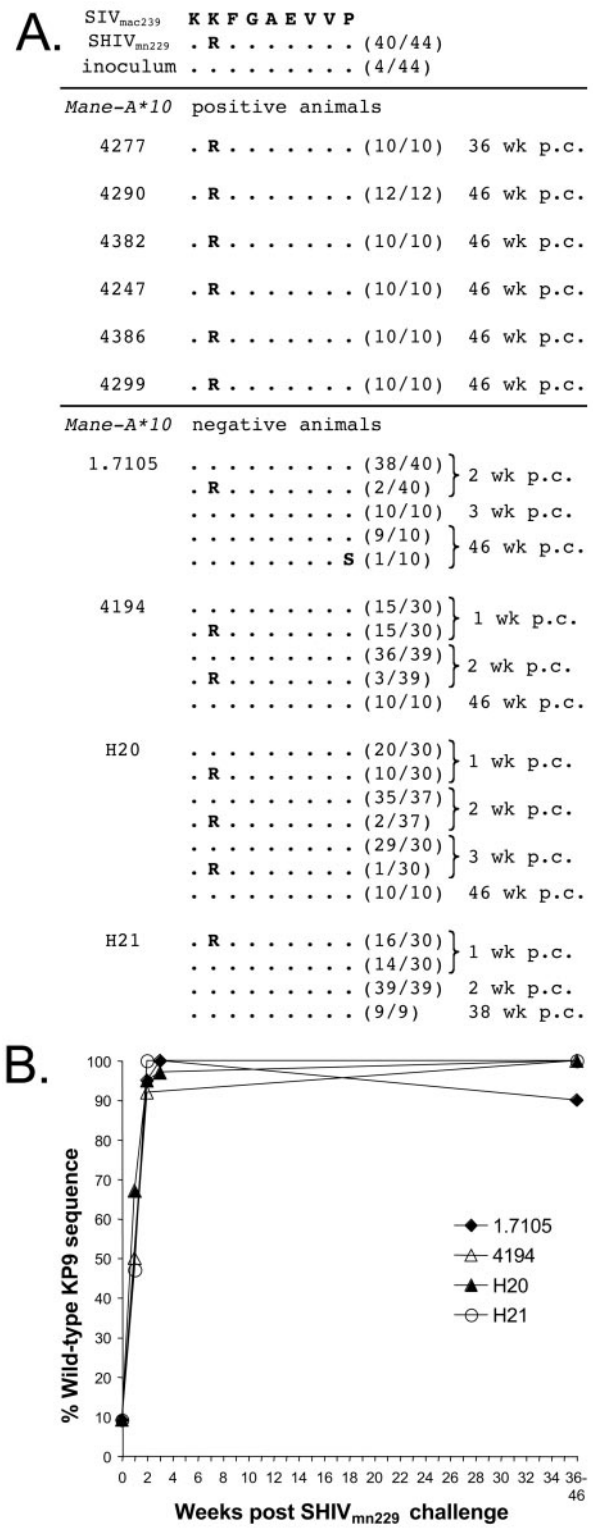

FIG. 6. Maintenance and reversion of KP9 escape mutations. (A) Predicted amino acid sequences across the KP9 epitope in multiple clones isolated at time points postchallenge (p.c.) with plasma $SHIV_{mn229}$ virus from KP9-responding animals (top panel) showing maintenance of K165R mutation at position 2 or KP9-nonresponding animals (bottom panel) showing reversion to the wild-type KP9 sequence. (B) Proportions of clones reverting to wild-type in KP9 nonresponders are shown graphically.

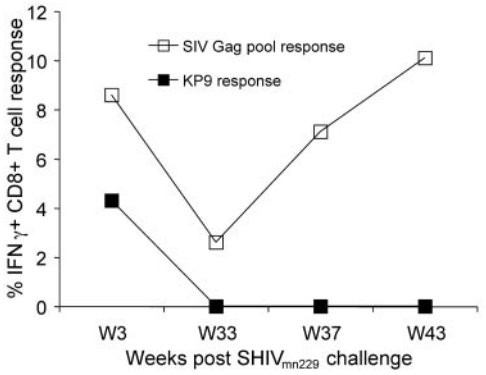

FIG. 7. Time course (by weeks [W]) of CD8 T-cell responses (positive for IFN-γ expression [IFNγ+]) to SIV Gag peptide pool or to KP9 epitope in KP9-responding animal 4290.

predominance of the K165R escape mutant in animal 95229 during the second challenge, we could not detect the *Mane-A*10* (or the closely related *Mane-A*16*) allele in this animal. Our data on the subsequent use of the passaged $SHIV_{mn229}$ virus as a challenge stock, for which rapid reversion occurs in the absence of KP9 presentation, suggest the possibility that this animal expresses another allele that can also present the KP9 epitope. Such "footprinting" of the virus by T-cell escape mutants has been advocated as a powerful tool to dissect T-cell epitopes (17, 20, 21). It is tempting to speculate that pathogenic SIV and SHIV challenge stocks previously passaged through rhesus macaques are also likely to have acquired T-cell escape mutations to epitopes restricted by common rhesus MHC alleles. Understanding the outcome of challenge with known, specific T-cell escape SIV or SHIV in macaques with particular MHC alleles mimicking most closely serial human transmission should lead to greater insights into the requirements for protective immunity to HIV.

The sequential appearance of the P172S and K165R mutations was observed both in the serial in vivo passage of the $SHIV_{HXB2}$ parent of the $SHIV_{mn229}$ virus as well as during de novo T-cell escape from $SHIV_{SF162P3}$ in two KP9-responding animals. The P172S mutation may initially reduce the significant fitness cost of the K165R mutation. We have also observed an additional Gag mutation, V145A, commonly detected at later time points in animals responding to KP9 (unpublished data) upstream from the KP9 epitope. Although this could represent another as yet unidentified epitope, this V145A mutation may represent a compensatory flanking mutation, as has been observed with other T-cell epitopes in humans and macaques (9, 10, 14, 17).

The use of the "preescaped" $SHIV_{mn229}$ stock as a challenge stock in vaccine trials is, to our knowledge, not previously reported. This may be a particularly difficult challenge virus for animals with Mane-A*10 to control, since the majority of the response is directed at this dominant epitope. On the other hand, effective, dominant CD8 T-cell epitopes generated in only a portion of outbred animals might skew the results of challenge studies, which have been described for the dominant SIV Gag epitope CM9 in Mamu-A*01-positive rhesus macaques (24). The use of preescaped challenge stocks may ne-

TABLE 3.. Estimated growth disadvantages of wild-type virus from published studies

Study subject (reference)	Frequency (day)[a]		Growth rate difference/day[b]	Half-life (h)[c]
	Initial	Final		
SIV_{mac239} (acute) Tat SL8 (1)	37/37 (14)	1/17 (28)	>0.45	<37
SHIV (chronic) Gag p11c (3)	8/8 (98)	0/10 (140)	>0.10	<166
HIV (acute) gp $160_{30–38}$ (5)	7/11 (30)	2/9 (44)	>0.13	<128
HIV (acute) Tat (6)	10/10 (34)	3/10 (51)	>0.18	<92
HIV (acute) Vpr (6)	12/12 (34)	5/10 (51)	>0.14	<118

[a] The initial and final frequencies of wild-type sequences at the indicated times were used to calculate the growth disadvantage of wild-type virus.
[b] Estimates shown are the minimum growth rate difference over these periods. More-frequent sampling may have increased these estimates.
[c] The half-life for increased CTL killing of wild-type virus compared with escape mutant virus (estimated from the difference in growth rates).

gate any dramatic advantage of dominant T-cell epitopes and represents an interesting virus challenge model.

The rapid selection of T-cell escape mutant virus in acute infection presents significant challenges for the development of vaccines for HIV. However, the high fitness costs of escape mutation also provide some reason for optimism. The usefulness of many T-cell responses may ultimately depend on the fitness cost associated with T-cell escape mutants. The rate of reversion of T-cell escape mutants in new hosts not able to respond to the same epitope provides an insight into the fitness cost associated with this escape variant. In the studies reported herein, we estimate, based on the near-complete replacement of K165R escape variants with wild-type virus across the KP9 epitope within 14 days in four animals, that the wild-type virus has an intrinsic growth advantage, with the ratio of wild-type to K165R mutant virus doubling every ~2 days. Similarly, the rate of replacement of wild-type with T-cell escape variants in subjects responding to an epitope allows an estimate of the growth advantage of the escape variant in the face of T-cell pressure. In this study, once escape was initiated at the K165R site (presumably a stochastic event and perhaps facilitated by the P172S mutant), at 2.5 or 3 weeks, rapid and near-complete replacement of wild type with K165R variants over 7 days ensued, indicative of a half-life of infected cells due to KP9-specific CTL of around 12.7 h. Interestingly, although the fact is anecdotal, the one KP9-responding animal that did not generate T-cell escape variants (animal 3790) effectively controlled SHIV viremia within 4 weeks following challenge (data not shown), likely resulting in the lack of sufficient viral replication to force T-cell escape. More-frequent sampling over these relative short time frames of escape and reversion should allow more accurate estimates of the growth advantages of wild-type and escape viral variants.

In summary, these detailed studies on escape and reversion at critical SHIV T-cell epitopes in pigtail macaques provide a powerful tool to analyze the impact of various T-cell immune responses on viral control. Defining and inducing the most effective T-cell immune responses against HIV should rationally improve the design of future vaccines.

ACKNOWLEDGMENTS

We thank Socheata Chea, Cara Riek, Richard Sydenham, and Jason Weinfurter for excellent technical support and Ruy Ribeiro for helpful comments.

This work was supported by Australian National Health and Medical Research Council grants 251653, 251654, and 299907 and NIH awards R24-RR-15371, R24-RR-016038, and P51-RR-00167643. M.P.D. is supported by the James S. McDonnell Foundation 21st Century Science Awards/Studying Complex Systems.

REFERENCES

1. **Allen, T. M., D. H. O'Connor, P. Jing, J. L. Dzuris, B. R. Mothe, T. U. Vogel, E. Dunphy, M. E. Liebl, C. Emerson, N. Wilson, K. J. Kunstman, X. Wang, D. B. Allison, A. L. Hughes, R. C. Desrosiers, J. D. Altman, S. M. Wolinsky, A. Sette, and D. I. Watkins.** 2000. Tat-specific cytotoxic T lymphocytes select for SIV escape variants during resolution of primary viraemia. Nature **407:** 386–390.
2. **Arguello, J. R., A. M. Little, E. Bohan, J. M. Goldman, S. G. Marsh, and J. A. Madrigal.** 1998. High resolution HLA class I typing by reference strand mediated conformation analysis (RSCA). Tissue Antigens **52:**57–66.
3. **Barouch, D. H., S. Santra, J. E. Schmitz, M. J. Kuroda, T. M. Fu, W. Wagner, M. Bilska, A. Craiu, X. X. Zheng, G. R. Krivulka, K. Beaudry, M. A. Lifton, C. E. Nickerson, W. L. Trigona, K. Punt, D. C. Freed, L. Guan, S. Dubey, D. Casimiro, A. Simon, M. E. Davies, M. Chastain, T. B. Strom, R. S. Gelman, D. C. Montefiori, and M. G. Lewis.** 2000. Control of viremia and prevention of clinical AIDS in rhesus monkeys by cytokine-augmented DNA vaccination. Science **290:**486–492.
4. **Bonhoeffer, S., A. D. Barbour, and R. J. De Boer.** 2002. Procedures for reliable estimation of viral fitness from time-series data. Proc. R. Soc. Lond. B **269:**1887–1893.
5. **Borrow, P., H. Lewicki, X. Wei, M. S. Horwitz, N. Peffer, H. Meyers, J. A. Nelson, J. E. Gairin, B. H. Hahn, M. B. A. Oldstone, and G. M. Shaw.** 1997. Antiviral pressure exerted by HIV-1-specific CTLs during primary infection demonstrated by rapid selection of CTL escape virus. Nat. Med. **3:**205–211.
6. **Cao, J., J. McNevin, U. Malhotra, and M. J. McElrath.** 2003. Evolution of CD8+ T cell immunity and viral escape following acute HIV-1 infection. J. Immunol. **171:**3837–3846.
7. **Dale, C. J., R. De Rose, I. Stratov, S. Chea, D. Montefiori, S. A. Thomson, I. A. Ramshaw, B. E. Coupar, D. B. Boyle, M. Law, and S. J. Kent.** 2004. Efficacy of DNA and fowlpox virus priming/boosting vaccines for simian/human immunodeficiency virus. J. Virol. **78:**13819–13828.
8. **Dale, C. J., X. S. Liu, R. De Rose, D. F. Purcell, J. Anderson, Y. Xu, G. R. Leggatt, I. H. Frazer, and S. J. Kent.** 2002. Chimeric human papilloma virus-simian/human immunodeficiency virus virus-like-particle vaccines: immunogenicity and protective efficacy in macaques. Virology **301:**176–187.
9. **Friedrich, T. C., E. J. Dodds, L. J. Yant, L. Vojnov, R. Rudersdorf, C. Cullen, D. T. Evans, R. C. Desrosiers, B. R. Mothe, J. Sidney, A. Sette, K. Kunstman, S. Wolinsky, M. Piatak, J. Lifson, A. L. Hughes, N. Wilson, D. H. O'Connor, and D. I. Watkins.** 2004. Reversion of CTL escape-variant immunodeficiency viruses in vivo. Nat. Med. **10**:275–281.
10. **Friedrich, T. C., C. A. Frye, L. J. Yant, D. H. O'Connor, N. A. Kriewaldt, M. Benson, L. Vojnov, E. J. Dodds, C. Cullen, R. Rudersdorf, A. L. Hughes, N. Wilson, and D. I. Watkins.** 2004. Extraepitopic compensatory substitutions partially restore fitness to simian immunodeficiency virus variants that escape from an immunodominant cytotoxic-T-lymphocyte response. J. Virol. **78:**2581–2585.
11. **Goulder, P. J., C. Brander, Y. Tang, C. Tremblay, R. A. Colbert, M. M. Addo, E. S. Rosenberg, T. Nguyen, R. Allen, A. Trocha, M. Altfeld, S. He, M. Bunce, R. Funkhouser, S. I. Pelton, S. K. Burchett, K. McIntosh, B. T. Korber, and B. D. Walker.** 2001. Evolution and transmission of stable CTL escape mutations in HIV infection. Nature **412:**334–338.
12. **Harouse, J. M., A. Gettie, T. Eshetu, R. C. Tan, R. Bohm, J. Blanchard, G. Baskin, and C. Cheng-Mayer.** 2001. Mucosal transmission and induction of simian AIDS by CCR5-specific simian/human immunodeficiency virus SHIV(SF162P3). J. Virol. **75:**1990–1995.
13. **Harouse, J. M., A. Gettie, R. C. Tan, J. Blanchard, and C. Cheng-Mayer.** 1999. Distinct pathogenic sequela in rhesus macaques infected with CCR5 or CXCR4 utilizing SHIVs. Science **284:**816–819.
14. **Kelleher, A. D., C. Long, E. C. Holmes, R. L. Allen, J. Wilson, C. Conlon, C. Workman, S. Shaunak, K. Olson, P. Goulder, C. Brander, G. Ogg, J. S. Sullivan, W. Dyer, I. Jones, A. J. McMichael, S. Rowland-Jones, and R. E.**

Phillips. 2001. Clustered mutations in HIV-1 gag are consistently required for escape from HLA-B27-restricted cytotoxic T lymphocyte responses. J. Exp. Med. **193:**375–386.

15. **Kent, S. J., A. Zhao, S. Best, J. D. Chandler, D. B. Boyle, and I. A. Ramshaw.** 1998. Enhanced T cell immunogenicity and protective efficacy of a human immunodeficiency virus type 1 vaccine regimen consisting of consecutive priming with DNA and boosting with recombinant fowlpox virus. J. Virol. **72:**10180–10188.
16. **Koup, R. A., J. T. Safrit, Y. Cao, C. A. Andrews, G. McLeod, W. Borkowsky, C. Farthing, and D. D. Ho.** 1994. Temporal association of cellular immune responses with the initial control of viremia in primary human immunodeficiency virus type 1 syndrome. J. Virol. **68:**4650–4655.
17. **Leslie, A. J., K. J. Pfafferott, P. Chetty, R. Draenert, M. M. Addo, M. Feeney, Y. Tang, E. C. Holmes, T. Allen, J. G. Prado, M. Altfeld, C. Brander, C. Dixon, D. Ramduth, P. Jeena, S. A. Thomas, A. St John, T. A. Roach, B. Kupfer, G. Luzzi, A. Edwards, G. Taylor, H. Lyall, G. Tudor-Williams, V. Novelli, J. Martinez-Picado, P. Kiepiela, B. D. Walker, and P. J. Goulder.** 2004. HIV evolution: CTL escape mutation and reversion after transmission. Nat. Med. **10:**282–289.
18. **Lu, Y., M. S. Salvato, C. D. Pauza, J. Li, J. Sodroski, K. Manson, M. Wyand, N. Letvin, S. Jenkins, N. Touzjian, C. Chutkowski, N. Kushner, M. LeFaile, L. G. Payne, and B. Roberts.** 1996. Utility of SHIV for testing HIV-1 vaccine candidates in macaques. J. Acquir. Immune Defic. Syndr. Hum. Retrovirol. **12:**99–106.
19. **Maecker, H. T., H. S. Dunn, M. A. Suni, E. Khatamzas, C. J. Pitcher, T. Bunde, N. Persaud, W. Trigona, T. M. Fu, E. Sinclair, B. M. Bredt, J. M. McCune, V. C. Maino, F. Kern, and L. J. Picker.** 2001. Use of overlapping peptide mixtures as antigens for cytokine flow cytometry. J. Immunol. Methods **255:**27–40.
20. **McMichael, A., and P. Klenerman.** 2002. HIV/AIDS. HLA leaves its footprints on HIV. Science **296:**1410–1411.
21. **Moore, C. B., M. John, I. R. James, F. T. Christiansen, C. S. Witt, and S. A. Mallal.** 2002. Evidence of HIV-1 adaptation to HLA-restricted immune responses at a population level. Science **296:**1439–1443.
22. **O'Connor, D. H., T. M. Allen, T. U. Vogel, P. Jing, I. P. DeSouza, E. Dodds, E. J. Dunphy, C. Melsaether, B. Mothe, H. Yamamoto, H. Horton, N. Wilson, A. L. Hughes, and D. I. Watkins.** 2002. Acute phase cytotoxic T lymphocyte escape is a hallmark of simian immunodeficiency virus infection. Nat. Med. **8:**493–499.
23. **O'Connor, D. H., B. R. Mothe, J. T. Weinfurter, S. Fuenger, W. M. Rehrauer, P. Jing, R. R. Rudersdorf, M. E. Liebl, K. Krebs, J. Vasquez, E. Dodds, J. Loffredo, S. Martin, A. B. McDermott, T. M. Allen, C. Wang, G. G. Doxiadis, D. C. Montefiori, A. Hughes, D. R. Burton, D. B. Allison, S. M. Wolinsky, R. Bontrop, L. J. Picker, and D. I. Watkins.** 2003. Major histocompatibility complex class I alleles associated with slow simian immunodeficiency virus disease progression bind epitopes recognized by dominant acute-phase cytotoxic-T-lymphocyte responses. J. Virol. **77:**9029–9040.
24. **Pal, R., D. Venzon, N. L. Letvin, S. Santra, D. C. Montefiori, N. R. Miller, E. Tryniszewska, M. G. Lewis, T. C. VanCott, V. Hirsch, R. Woodward, A. Gibson, M. Grace, E. Dobratz, P. D. Markham, Z. Hel, J. Nacsa, M. Klein, J. Tartaglia, and G. Franchini.** 2002. ALVAC-SIV-gag-pol-env-based vaccination and macaque major histocompatibility complex class I (A*01) delay simian immunodeficiency virus SIVmac-induced immunodeficiency. J. Virol. **76:**292–302.
25. **Phillips, R. E., S. Rowland-Jones, D. F. Nixon, F. M. Gotch, J. P. Edwards, A. O. Ogunlesi, J. G. Elvin, J. A. Rothbard, C. R. Bangham, C. R. Rizza, et al.** 1991. Human immunodeficiency virus genetic variation that can escape cytotoxic T cell recognition. Nature **354:**453–459.
26. **Richman, D. D., T. Wrin, S. J. Little, and C. J. Petropoulos.** 2003. Rapid evolution of the neutralizing antibody response to HIV type 1 infection. Proc. Natl. Acad. Sci. USA **100:**4144–4149.
27. **Russell, N. D., M. G. Hudgens, R. Ha, C. Havenar-Daughton, and M. J. McElrath.** 2003. Moving to human immunodeficiency virus type 1 vaccine efficacy trials: defining T cell responses as potential correlates of immunity. J. Infect. Dis. **187:**226–242.
28. **Schmitz, J. E., M. J. Kuroda, S. Santra, V. G. Sasseville, M. A. Simon, M. A. Lifton, P. Racz, K. Tenner-Racz, M. Dalesandro, B. J. Scallon, J. Ghrayeb, M. A. Forman, D. C. Montefiori, E. P. Rieber, N. L. Letvin, and K. A. Reimann.** 1999. Control of viremia in simian immunodeficiency virus infection by CD8+ lymphocytes. Science **283:**857–860.
29. **Smith, M. Z., C. J. Dale, R. De Rose, I. Stratov, C. S. Fernandez, A. G. Brooks, J. T. Weinfurter, K. Krebs, C. Riek, D. I. Watkins, D. H. O'Connor, and S. J. Kent.** 2005. Analysis of pigtail macaque major histocompatibility complex class I molecules presenting immunodominant simian immunodeficiency virus epitopes. J. Virol. **79:**684–695.
30. **Thompson, J., S. L. Hu, L. Kuller, B. Travis, W. R. Morton, and M. B. Agy.** 1996. SHIVIIIB infection of Macaca nemestrina: determination of a macaque infectious dose. 11th Int. Conf. AIDS, abstr. We.A. 142, p. 5.
31. **Thompson, J. L., D. Anderson, J. Ranchalis, L. Kuller, H. Mack, and M. B. Agy.** 2000. Intravaginal titration of the acutely pathogenic SHIV229 in Macaca nemestrina. J. Med. Primatol. **29:**295.
32. **Wei, X., J. M. Decker, S. Wang, H. Hui, J. C. Kappes, X. Wu, J. F. Salazar-Gonzalez, M. G. Salazar, J. M. Kilby, M. S. Saag, N. L. Komarova, M. A. Nowak, B. H. Hahn, P. D. Kwong, and G. M. Shaw.** 2003. Antibody neutralization and escape by HIV-1. Nature **422:**307–312.